

HD 99458: First time ever Ap-type star as a δ Scuti pulsator in a short period eclipsing binary?*

M. Skarka,^{1,2†} P. Kabáth,² E. Paunzen,¹ M. Fedurco,³ J. Budaj,⁴ D. Dupkala,^{2,5} J. Krτίčka,¹ A. Hatzes,⁶ T. Pribulla,⁴ Š. Parimucha,³ Z. Mikulášek,¹ E. Guenther,⁶ S. Sabotta,⁶ M. Blažek,^{1,2} J. Dvořáková,^{2,7} L. Hambálek,⁴ T. Klocová,² V. Kollár,⁴ E. Kundra,⁴ M. Šlechta,² and M. Vaňko⁴

¹Department of Theoretical Physics and Astrophysics, Masaryk University, Kotlářská 2, 61137 Brno, Czech Republic

²Astronomical Institute, Czech Academy of Sciences, Fričova 298, 25165, Ondřejov, Czech Republic

³Faculty of Science, P. J. Šafárik University, Park Angelinum 9, Košice 04001, Slovak Republic

⁴Astronomical Institute, Slovak Academy of Sciences, 05960 Tatranská Lomnica, Slovak Republic

⁵Astronomical Institute, Charles University, Faculty of Mathematics and Physics, 18000 Praha 8, V Holešovičkách 2, Czech Republic

⁶Thüringer Landessternwarte Tautenburg, Sternwarte 5, 07778 Tautenburg, Germany

⁷Institute of Physics, Faculty of Philosophy and Science, Silesian University in Opava, Bezručovo nám. 13, 74601 Opava

Accepted XXX. Received YYY; in original form ZZZ

ABSTRACT

We present the discovery of a unique object, a chemically peculiar Ap-type star showing δ Scuti pulsations which is bound in an eclipsing binary system with an orbital period shorter than 3 days. HD 99458 is, therefore, a complex astrophysical laboratory opening doors for studying various, often contradictory, physical phenomena at the same time. It is the first Ap star ever discovered in an eclipsing binary. The orbital period of 2.722 days is the second shortest among all known chemically peculiar (CP2) binary stars. Pulsations of δ Scuti type are also extremely rare among CP2 stars and no unambiguously proven candidate has been reported. HD 99458 was formerly thought to be a star hosting an exoplanet, but we definitely reject this hypothesis by using photometric observations from the *K2* mission and new radial velocity measurements. The companion is a low-mass red dwarf star ($M_2 = 0.45(2)M_\odot$) on an inclined orbit ($i = 73.2(6)$ degrees) that shows only grazing eclipses. The rotation and orbital periods are synchronized, while the rotation and orbital axes are misaligned. HD 99458 is an interesting system deserving of more intense investigations.

Key words: techniques: photometric – techniques: spectroscopic – binaries: eclipsing – stars: chemically peculiar – stars: oscillations – stars: individual: HD 99458

1 INTRODUCTION

Chemically peculiar stars of the upper part of main sequence are usually slowly rotating stars where the processes of radiative diffusion and gravitational settling lead to abundance anomalies (Michaud et al. 1976). Because these diffusion processes are typically very slow, the atmospheres of chemically peculiar stars should be stable against mixing processes caused by, for example, rotation, binary interaction, stellar wind and convection.

A class of chemically peculiar stars called CP2 is characterized by overabundance of heavy elements, frequent ap-

pearance of magnetic field, and slow rotation (Preston 1974). Heavy elements on the surface of CP2 stars concentrate in vast abundance spots that result in spectroscopic and light variability. Chemically peculiar stars show rotational modulation of the light curve that is due to the flux re-distribution in the abundance spots (e.g. Prvák et al. 2015).

Although the overall frequency of CP2 binaries is relatively high (Carrier et al. (2002) give 43%, Mathys (2017) gives 51%), this distribution is dominated by long-period systems. There appears to be a significant deficiency of systems with period of the order days to tens of days and a complete lack of binaries with period below 2.9 days (Carrier et al. 2002; Mathys 2017; Landstreet et al. 2017). As a result, eclipsing binary systems are absent in the sample

† E-mail: maska@physics.muni.cz

of known CP2 stars, which complicates the determination of stellar parameters and evolutionary stage of these stars. According to Ferrario et al. (2009) and Tutukov & Fedorova (2010), the presence of magnetic fields and lack of close binaries can be a result of the merger process. Consequently, a discovery of a CP2 in eclipsing binary would imply that the merger scenario cannot account for the origin of the magnetic field in all cases.

HD 99458 (EPIC 201534540, J2000 RA=11^h36^m36.28^s, DEC=+01°03′18.84″, $V = 8.163$ mag, $(B - V) = 0.241$ mag) was identified as a transiting exoplanetary candidate with period of $P = 2.722$ d by Barros et al. (2016). In this brief note, we show that the companion must be of stellar nature. We investigate the spectra and light curve and show that in terms of stellar physics this is an extremely interesting star. To our knowledge, this is the first discovery of its kind that can point us towards a better understanding of the A-type stars and their chemically peculiar subclass.

2 DATA

HD 99458 was observed in campaign 1 of the *K2* mission (Howell et al. 2014). We used the single-aperture light-curve (hereafter LC) data. The data set has a time span of 80 days and contains 3500 data points taken with an integration time of 29.4 minutes. For an easier handling we normalized the flux to 700 000 e-/s.

To validate the nature of the transits, we gathered 58 spectra in 2017 and 2018 with the Ondřejov Echelle Spectrograph (OES) mounted at the 2-m Perek telescope at the Ondřejov observatory, Czech Republic. This spectrograph has a resolving power $R = \lambda/\Delta\lambda = 50000$ (Koubský et al. 2004). Additional observations were taken with the fibre-fed echelle spectrograph mounted at the 60-cm telescope at Stará Lesná Observatory, Slovak Republic ($R = 11000$, Pribulla et al. 2015).

The typical S/N ratio was between 20 and 80 depending on the observing conditions and the air mass. The data were reduced with the standard IRAF 2.16 routines¹ (Tody 1993). For the estimation of radial velocities we used IRAF FXCOR routine. To minimize the effects of data reduction and calibration, we cross-correlate the lines in 13 subsequent overlapping regions with the width of 100 Å between 4900 and 5500 Å. As a template, one of the best quality spectrum was selected. The instrumental shift was removed using telluric lines. The resulting radial velocities calculated as the weighted mean of the values assuming the weights based on the uncertainties provided by FXCOR were shifted with respect to their mean. Thus, we give only relative radial velocities (RVs) in Table A2.

3 DATA ANALYSIS

To make all the performed procedures in binary modelling easier to follow, we summarise the steps here. First, we get

the effective temperature, surface gravity, mass and radius of the primary on the basis of astrometry, photometric and spectroscopic observations, without considering it as a binary member. These parameters are then fixed and used as inputs for the next steps of the procedure. Other parameters of the primary are also derived at this stage, such as $v \sin i$ and v_{mic} , but they are not relevant for the next steps of binary modelling.

The RV data are analysed to compute an orbital solution according to the standard procedure for spectroscopic binaries. Value of the orbital period was determined from our RV measurements, while the epoch of the phase origin was adopted from literature. Among the parameters derived at this stage, the RV semi-amplitude and the mass function are fixed and used as input for the next step.

The light curve is modelled to derive the following parameters of the secondary: effective temperature, mass and radius, as well as the inclination of the orbital plane.

3.1 Physical characteristics

First of all, we estimated the reddening, T_{eff} , and $\log L/L_{\odot}$. The parallax from the Gaia DR2 is given as $\pi = 3.7774(699)$ mas which translates to a distance of 265 pc (Lindgren et al. 2018). The reddening was assumed to be zero (Green et al. 2018). Note that the Gaia DR2 lists a value of $E(B - V) = 0.1$ mag which seems to be too high. As the next step, we derived the T_{eff} using photometric colors. We have used the BV data published by Kharchenko (2001). The JHK_s magnitudes were taken from the 2MASS 6X Point Source Working Database (Skrutskie et al. 2006). The standard relations were taken from the updated list by Pecaú & Mamajek (2013). All colors give consistent values between 7 500 and 7 700 K, respectively. Again, the value in the Gaia DR2 of 8 199 K seems to be too high². Assuming the bolometric correction taken from Flower (1996), we get a bolometric luminosity $\log L/L_{\odot} = 1.52(2)$. From the luminosity and the evolutionary tracks from Bressan et al. (2012), we estimated $\log g = 3.70(5)$.

For the investigation of the metallicity and the projected rotational velocity $v \sin i$ of the primary, synthesized spectra were computed using the program SPECTRUM³ (Gray & Corbally 1994) and modified versions of the ATLAS9 code taken from the Vienna New Model Grid of Stellar Atmospheres, NEMO⁴ (Heiter et al. 2002). We used a stellar atmosphere with $T_{\text{eff}} = 7 600$ K, $\log g = 3.6$, and $v_{\text{mic}} = 2 \text{ km s}^{-1}$.

The synthetic spectrum was first convolved with the instrumental profile and then with different rotational profiles yielding a best fit for a $v \sin i$ of 50 km s^{-1} with an uncertainty of about 2 km s^{-1} . To test the astrophysical parameters derived from photometry, a grid of atmospheres with effective temperatures and surface gravities around the input values were applied. The hydrogen lines are best fitted with the values mentioned above with the assumption that they are

¹ IRAF is distributed by the National Optical Astronomy Observatories, which are operated by the Association of Universities for Research in Astronomy, Inc., under cooperative agreement with the National Science Foundation.

² See Table A1 for comparison of the parameters available in the current literature.

³ <http://www.appstate.edu/~grayro/spectrum/spectrum.html>

⁴ <http://www.univie.ac.at/nemo>

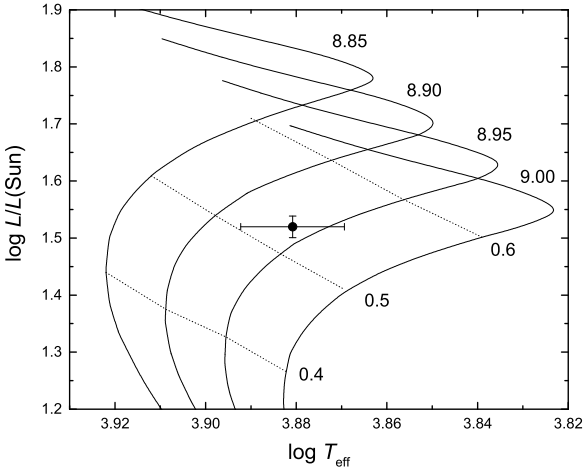


Figure 1. The location of the primary component within the $\log L/L_{\odot}$ versus $\log T_{\text{eff}}$ diagram. The isochrones with \log values from 8.85 to 9.0 were taken from Bressan et al. (2012). Lines of constant $\log R/R_{\odot}$ values are also included.

not sensitive to $\log g$. Also the overall metallic line spectrum is well fitted. For spectra cooler than 7400 K, many lines appear which are not visible in the observed stellar spectrum. We have to emphasize that also a spectrum of 8000 K fits the metallic line spectrum, but this would mean that the abundances anomalies are even more pronounced because the overall metallic line spectrum gets weaker for hotter temperatures.

To estimate the $[Z/H]$ values for the individual elements, we used different models with metallicities from +2 to -1 dex. Then we compared all the individual lines of one element to the synthetic spectra resulting in a mean value for each traceable element with an heuristic error of about ± 0.2 dex. We found that Fe, Si, and Ti are overabundant with $> +1$ dex compared to solar abundance, while Ca, Mn, Ni and Y are slightly overabundant (from +0.2 to +0.8 dex). Such an abundance pattern is typical for magnetic Ap (CP2) stars (Bailey et al. 2014).

As the last step, we estimated the mass, radius and age of the primary component using the isochrones by Bressan et al. (2012) and the values listed above. A two-dimensional interpolation within this grid yields $M_1 = 2.15(5) M_{\odot}$, $\log R/R_{\odot} = 0.54(2)$, and $\log t = 8.93(5)$ years (see Fig. 1). The star is clearly a main-sequence star. Using the formula for rigid body rotation (assuming the period $P = 2.722$ d and radius $R = 3.467 R_{\odot}$), applied for chemically peculiar stars (Paunzen & Maitzen 1998), we derived an equatorial rotational velocity V_{eq} of $64(2) \text{ km s}^{-1}$ and an inclination i of $50(2)^{\circ}$.

3.2 Binary model

Since the time base of our RV data is more than ten-times larger than photometric data from *K2*, we were able to improve the orbital period. For phasing the data (Figs. 2 and 3) we used the ephemeris:

$$T_{\text{min}} = 2456814.4918 + 2.722045(9) \times E. \quad (1)$$

The zero epoch was taken from (Barros et al. 2016).

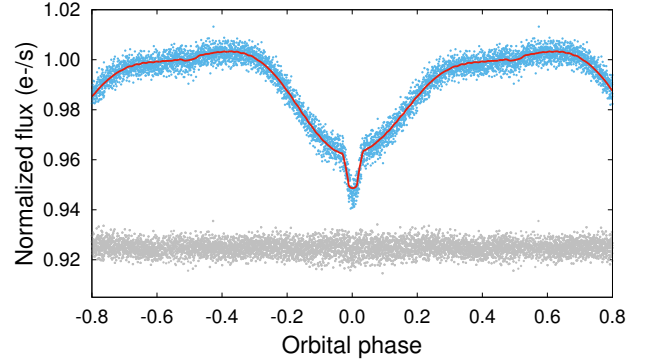


Figure 2. Photometric data phased according to eq. 1. The solid line shows the PHOEBE fit assuming two dark spots on the surface. The grey points in the bottom part of the figure show the residuals (RMS $\sim 0.003 \text{ e-/s}$).

The *K2* data shows smooth variations in brightness. There is a broad dip between phases -0.3 and 0.3 with an amplitude of about 4% (normalized flux between approx. 0.96 and 1.01 in Fig. 2) and a sudden, 0.18-d long, 1.5% drop at phase 0.0 which is caused by the transiting small companion (we will call it transit). At phase 0.5 the secondary eclipse is apparent.

We assume that the changes out of the transit are due to photometric spot(s) on the surface of the primary star combined with the binary proximity effects (ellipticity of the components, possible reflection effect etc.). These phenomena cannot be easily distinguished from the broad-band long-cadence *K2* data itself, but multicolour photometry and high-resolution and high-SNR spectra that are currently unavailable would help in future. In Sect. 3.3, we investigate the residuals shown in the bottom part of Fig. 2 and identify short-period variations, probably arising from pulsations.

Analysis of the RV data (Fig. 3) including the use of RADVEL software (Pribulla et al. 2015) yielded a semi-amplitude of $K = 35.2(3) \text{ km s}^{-1}$ and a mass function $f(M) = 0.0123(3) M_{\odot}$, which were together with the parameters from sect. 3 (see Table A1) fixed and used as the input parameters for the light-curve model in PHOEBE (ver. 0.31, Prsa et al. 2011).

We fixed the eccentricity to zero, because primary and secondary minima always occur at phases 0.0 and 0.5⁵. We also kept the effective temperature of the primary component fixed at 7600 K (derived from spectroscopy). Values of gravity darkening and albedo for the primary component were fixed to 1 because the effective temperature indicates the presence of radiative envelope (Claret 1999). Because we expected a smaller and colder companion we fixed the albedo of the secondary component to 0.6 and the gravity darkening factor to 0.32 which are corresponding values for a convective envelope. A linear cosine law for limb darkening was used, with coefficients interpolated from van Hamme (1993) tables. During the whole procedure we constrained the mass,

⁵ RADVEL gives $e = 0.008 \pm 0.008$.

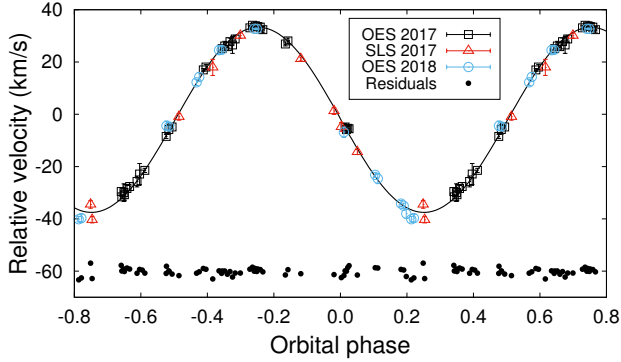


Figure 3. The radial velocity curve showing measurements from the two observing facilities in 2017 and 2018, the fit obtained with RADVEL (the solid line), and the residuals (black dots around -60 km s^{-1}). SLS means Stará Lesná Spectrograph.

surface gravity and radius of the primary component to the values obtained from spectroscopy⁶.

To get the starting values for the binary model, we first removed the main, out-of-transit photometric variations by modelling them with two-component harmonic polynomial⁷. Such photometric residuals were fitted simultaneously with the RV observations. However, due to the fact that the pre-whitening procedure discarded all the information about ellipsoidal variations caused by tidally deformed components, we decided to fit the eclipsing binary model only with LC data in immediate vicinity of transit and secondary eclipse. This resulted in poor estimate of temperature of the secondary component, which we fix to 3700 K consistent with the radius and mass of the secondary (see below). After the first-order estimation of the input parameters of the secondary component, we modelled the original data by assuming two spots on the surface of the primary. The resulting model is shown with continuous line in Fig. 2. This is, of course, a huge simplification because spots on the surface of CP stars are not temperature spots but rather abundance spots having a different chemical composition than the surrounding photosphere (e.g. Prvák et al. 2015). Nevertheless, it demonstrates well that the variations can be parametrized using two spots on the surface.

The secondary is a small star on a circular orbit that makes a grazing eclipse (transit). Our model gives $M_2 = 0.45(2) M_\odot$, $R_2 = 0.59 R_\odot$, $i = 73.2(6)^\circ$. The full set of parameters is shown in Table 1. We conclude the secondary is an early M-type main-sequence star with an bolometric magnitude of about +8 mag (Pecaut & Mamajek 2013) which is about 6.5 mag fainter than the primary. The light contribution of the secondary component has no significant effect on the overall absolute magnitude and thus the luminosity.

If we assume that the rotational axis is aligned with the orbital axis ($i = 73.2(6)^\circ$), we derive $V_{\text{eq}} = 52 \text{ km s}^{-1}$ and $\log R/R_\odot = 0.45$ for the primary star, respectively. The latter is clearly not compatible with the isochrones (Fig. 1). This

⁶ The values stay within errors when they are left as free parameters during the fitting process.

⁷ The same result can be achieved by using 10-th order algebraic polynomial.

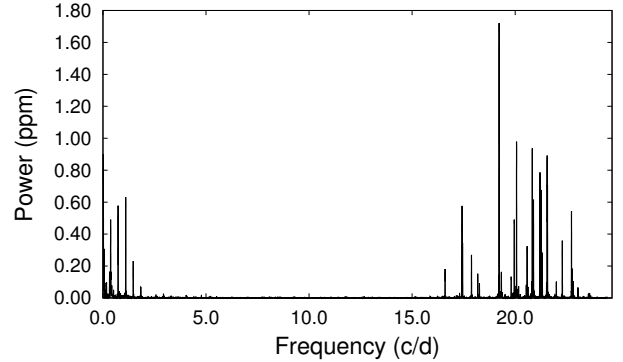


Figure 4. Power spectra of the residuals after the binary model was removed. The low-frequency peaks are relics of the orbital period, while the peaks around 20 c/d are real manifestations of pulsations of δ Scuti type.

implies that the rotational axis is misaligned by about 20° to the orbital axis. However, because the primary minimum and the out-of-transit variations have minimum always in phase 0, the orbital and rotational period of the primary star are equal.

3.3 Pulsations

In the previous section we obtained good fit of the light curve assuming binary model with spots on the primary. In the next step we subtracted this fit from the observations and performed a frequency analysis on photometric residuals using PERIOD04 (Lenz & Breger 2005). The power spectrum (Fig. 4) shows a series of peaks at low frequencies which are most likely artifacts due to instrumental effects and the orbital frequency and its harmonics. We attribute the cluster of peaks around 20 c/d to stellar variability. However, we cannot fully rule out that some of these peaks (but not all) are artifacts of removing the binary model.

The highest peak at 19.2 c/d with amplitude of 1.28 ppt (in the power spectra $\sim 1.64 \text{ ppm}$) corresponds to the photometric variation with period of 1.25 hour. We identified at least six independent frequencies which we give in Table 2. Photometric variations of amplitudes $\sim \text{mmag}$ at frequencies higher than 5 c/d are typical for δ Scuti stars (Breger 2000). Therefore, the most natural explanation is that HD 99458 is a pulsating star of the δ Scuti type. However, other explanations are possible (see sect. 4.2 and 4.5). We do not explore further the pulsations because the long integration time of the data averages the short-time variations significantly.

4 DISCUSSION

4.1 Impact of fast rotation on the RV determination

The projected rotational velocity $v \sin i = 50 \text{ km s}^{-1}$ is larger than the semi-amplitude of the RV curve (Fig. 3), which raise question how the rotation influences the radial-velocity determination. First, RVs are measured using cross-correlation function method over a broad spectral region between 4900 and 5500 Å. The Si, Ti and lines of other over-

Table 1. Ephemerides and results from the binary fitting.

P (d)	2.722045(9)	fixed	$f(M)$ (M_{\odot})	0.0123(3)	fixed
T_0 (HJD)	2456814.4918	fixed	R_1 (R_{\odot})	3.47(16)	fixed
a (R_{\odot})	11.28(5)		R_2 (R_{\odot})	$0.59^{+0.06}_{-0.14}$	
$q = M_2/M_1$	0.21(1)		$\log g_1$ (cgs)	3.70(5)	fixed
K_1 (km s^{-1})	35.2(3)	fixed	$\log g_2$ (cgs)	4.55(5)	
i (deg)	73.2(6)		Spot1		
e	0	fixed	Longitude (deg)	130	
$T_{\text{eff}1}$ (K)	7600(100)	fixed	Colatitude (deg)	297	
$T_{\text{eff}2}$ (K)	3700	fixed	Radius (deg)	90	
$\Omega(L_1)$	2.26		$T_{\text{spot}1}/T_{\text{eff}1}$	0.9823	
$\Omega(L_2)$	2.13		Spot2		
Ω_1	3.52	fixed	Longitude (deg)	18.5	
Ω_2	$5.4^{+1.0}_{-0.5}$		Colatitude (deg)	65	
M_1 (M_{\odot})	2.15(5)	fixed	Radius (deg)	46	
M_2 (M_{\odot})	0.45(2)		$T_{\text{spot}2}/T_{\text{eff}1}$	0.943	

Table 2. First six independent frequencies identified in the δ Scuti regime. The corresponding errors in the last digits are in parentheses.

Frequency (c/d)	Amplitude (ppt)	Phase (rad)
19.22089(31)	1.28(6)	3.252(45)
20.06710(40)	0.99(6)	0.072(57)
20.83067(40)	0.98(6)	0.696(58)
21.55110(43)	0.92(6)	0.906(62)
21.20216(43)	0.92(6)	0.729(62)
21.26344(47)	0.83(6)	1.472(69)

abundant elements are fewer compared to other lines in the region (mainly Fe lines). These few lines cannot influence the final RV measurements.

Rotational modulation of 50 km s^{-1} would need that large chemical spots are both at the opposite edges of the disc, thus, their projected surfaces would be very small compared to the full disc area meaning no influence on the RV. Spots would need to be extremely large to have some impact on RV measurements.

The LC (Fig. 2) shows a maximum amplitude of 4%. For Ap stars and their chemical spots it is difficult to estimate the RV variations due to rotational modulation. For simplicity, let's assume that the photometric variations come from cool spots. We can then use the estimate of the RV amplitude of spots from Saar & Donahue (1997):

$$A_{\text{spot}} \sim 6.5 f_{\text{spot}}^{0.9} \nu \sin i, \quad (2)$$

where f_{spot} is the relative area of the spot in per cent and $\nu \sin i$ is in km s^{-1} .

For a photometric amplitude of 2% this corresponds to an RV amplitude of approximately 0.6 km s^{-1} , or only about 2% of the RV semi-amplitude. This translates into a change in stellar mass of the primary by the same amount. It is impossible that rotational modulation would account for a significant part of the RV variations as this would have resulted in much larger variations in the LC.

4.2 Contamination by nearby stars

Since HD 99458 is a unique object, all the observed features must be unambiguously confirmed to come from HD 99458. One possibility is that some of the features (e.g. δ Scuti vari-

ations) come from either of a few faint contaminants in the *K2* aperture. The brightest one is UCAC4 456-050614 which is 6 mag fainter than HD 99458 in *V* and is 1.5 arcmin apart from it⁸. We can safely exclude all the close stars as the source of the out-of-transit photometric variations because RVs correspond exactly to the photometric variations.

We can also exclude UCAC4 456-050614 as a source of oscillations because it has $(B-V) = 0.709$ (Zacharias et al. 2013), which is out of range for δ Scuti pulsations. However, in some circumstances, the (semi)periodic minutes-to-hours long variations could be due to granulation. If we consider the above mentioned colour, $V = 14.081$ mag (Zacharias et al. 2013), $\pi = 1.453$ mas (Gaia Collaboration et al. 2018), using standard relations from Pecaute & Mamajek (2013) we find that UCAC4 456-050614 is a solar analogue with temperature of about 5590 K.

By using the scaling relations from Samadi et al. (2013a,b) summarized in Cranmer et al. (2014), we get the maximal amplitude of the possible photometric variations as 0.05 ppt, which is orders of magnitude less than the amplitude of the observed variations (> 1 ppt). Thus granulation cannot explain the short-time variations either. A possible blend with a 14-mag star will also not impact the total amplitude of the photometric variations.

4.3 Origin of the out-of-transit photometric variations

Our analysis (sect. 3.1) shows that the primary component of HD 99458 is a chemically peculiar star of CP2 type (Preston 1974)⁹. This means that the surface is stratified due to different atomic diffusion rate of different elements (Michaud et al. 1976). Regions (spots) with different chemical abundances (typically iron-peak elements and Si, SrCrEu group of elements) can produce strictly periodic photometric variations due to rotation. To create and maintain chemical peculiarity in CP2 stars, a very stable atmosphere supported by the presence of strong large-scale globally-organized magnetic fields is required (Niemczura et al. 2014).

We suppose that the out-of-transit variation (see Fig. 2)

⁸ The other stars are fainter than 19 mag in *B*.

⁹ About 15-20% of B-F stars are CP stars (Romanyuk 2007).

is caused by chemical spots. We do not know the exact size and location of the spots because the models are ambiguous. One-spot model gives only a bit worse fit to the data than two-spot model. Without having multicolour photometry and high-resolution and high-SNR spectroscopy for line profile variation investigation we cannot say much more.

As an alternative explanation of the out-of-transit variations we considered the presence of a cool accretion disc and cool companion filling its Roche lobe which feeds the accretion disc. The eclipse of the disc would then produce the out-of-transit variations. We modeled the LC with SHELLSPEC code (Budaj & Richards 2004). The geometry of the Roche lobe which intersects the orbital plane in the L1 point at an angle of about $115 \pm 1\%$ degrees (Plavec & Kratochvíl 1964) gives an upper limit for the duration of the eclipse as 0.32 in phase. Thus, we are unable to reproduce the very broad main drop in flux which lasts about 0.5 in phase. At the same time it is very difficult to reproduce a relatively shallow major flux depression with the mass ratio of 0.21.

Additional structures or effects would have to be invoked. One possibility is that the two stars are surrounded by an optically thin cooler material located between the C1 and C2 Roche potential surfaces. We tried to model such an envelope as well but, unfortunately, we were not able to reproduce the observed light curve assuming the mass ratio of 0.21. Also, if such a disk were present in the system it might be seen in the form of a double peak emission in the strong lines such as H α . However, there is no clear evidence for such emission. Thus, the spot model is far more likely than such a disk model.

4.4 Binarity

Binarity among CP stars is still not well understood. Among non-magnetic metallic-line enhanced (CP1) and non-magnetic mercury-manganese (CP3) stars, the binary fraction is about 70 and 90%, respectively (Carquillat & Prieur 2007; Schöller et al. 2010). Among CP2 stars, the fraction of binary systems with long periods is similar to other A-type stars but only very few non-eclipsing SB binaries with periods less than 50 days have been discovered (Abt & Snowden 1973; Carrier et al. 2002; Mathys 2017; Landstreet et al. 2017). The only known binary with period below 3 days is HD 200405, which is non-eclipsing SB1 (Carrier et al. 2002). Concerning eclipsing binaries, there are two candidates containing a Bp star: V772 Cas (Gandet 2008, period 5 days) and HD 66051 (Paunzen et al. 2018; Kochukhov et al. 2018, period 4.7 days), which both have ambiguous Bp classification. The lack of CP2 stars bound in close binary systems may be due to an interplay between binarity and magnetism which prevents Ap occurring in such binaries (Abt & Snowden 1973; Budaj 1999). HD 99458 represents an ideal laboratory for investigations of binary-magnetism relation, can shed some light on how the magnetic field influences formation of close binary pairs, and how the chemical anomalies are related to the presence of the companion.

HD 99458 can be used to test the hypothesis of forming CP2 stars in close binaries via merging (Ferrario et al. 2009; Tutukov & Fedorova 2010). It could hardly be formed via merging since it would require formation and existence of three stars on very close orbits. Such systems are dynamically unstable. Moreover, the third body (the cur-

rent secondary component) would be probably kicked off further away by gaining the excess momentum from the merger process. HD 99458 is not the only known such star. Mathys (2017) listed several other short-period Ap binaries (HD 5550, HD 25267, HD 25823, HD 98088) and mentioned that the merging mechanism might not account for their formation. Tutukov & Fedorova (2010) also acknowledge the other process for the formation of Ap stars. Thus, HD 99458 is an additional example and argument for the existence of other channels of Ap star formation. However, this does not exclude the possibility that Ap stars that are not in close binaries have formed through merging.

4.5 Presence of pulsations

In the region of Hertzsprung-Russel diagram, where A-F main sequence stars are located, pressure (p) and gravity (g) modes can be excited and produce rapid oscillations, δ Scuti and γ Doradus type pulsations. In a few tens of CP2 stars, rapid oscillations with very short periods on the order of 5-20 minutes have been observed (roAp stars, Kurtz & Martinez 2000; Smalley et al. 2015). Recently, Bowman et al. (2018) analysed *K2* data of CP2 stars in order to investigate rotational and additional variability. In six of their sample stars they found additional variations possibly caused by pressure and gravity modes but their results are not conclusive.

HD 99458 clearly shows fast photometric variations that can be hardly explained in other way than by δ Scuti-type oscillations (see Fig. 4 with the dominant frequency at 19.2 c/d). A simple test with granulation on the secondary component by considering values from Table A1 would yield maximal possible amplitude of 0.018 ppt, which is also orders of magnitude less than the observed amplitude. Because blends and granulation can be rejected as the origin of the fast variations, and artificial origin of all the peaks is unlikely, we conclude that the observed δ Scuti variations are intrinsic to HD 99458 and are likely caused by the pulsations. The presence of δ Scuti oscillations makes HD 99458 unique object which can help investigate simultaneous presence of anomalous chemical composition in unstable atmospheric conditions.

5 SUMMARY AND FUTURE PROSPECTS

This short paper represents a brief investigation of a new class of objects represented by HD 99458. The aim is to bring the attention to this star and stimulate the observational follow-up efforts. We unambiguously proved that HD 99458 is a binary system consisting of A-type star and low-mass red dwarf, not a system hosting an exoplanet. The rotation and orbital periods are synchronous, however the rotation and orbital axes are misaligned by about 20 degrees. We clearly detected fast photometric variations that we attribute to pulsations of δ Scuti type that are intrinsic to the primary component.

HD 99458 shows spectacular out-of-transit variations, which we interpret as due to chemical spots on the surface of the primary star. Analysis of our spectra indicates that HD 99458 is a chemically peculiar star of CP2 type. As such,

it would be the first Ap star in a short-period eclipsing binary system. We discovered a unique astrophysical laboratory where various physical phenomena co-exist and can be studied simultaneously.

The available spectra and photometric data that were analysed allow only a very basic analysis. This study is just the beginning. Future high-SNR and high-resolution spectroscopy together with multicolour photometry will allow for better investigation of the chemical composition, distribution of the elements on the surface and the sizes of spots. Such observations will also help to disentangle the variations caused by spots and by proximity effects in the binary system, which are mixed and hard to distinguish because of synchronous rotation. High-cadence spectra and photometry will help to unambiguously confirm and better describe the pulsations. Spectropolarimetric series will allow for detection and orientation of the magnetic field and its variations. Such observations have already started and will be subject of a future paper.

ACKNOWLEDGEMENTS

We would like to thank all the technical staff that makes the observations possible. We are grateful to the anonymous referee who helped to improve the manuscript. We acknowledge SIMBAD and VizieR catalogue databases, operated at CDS, Strasbourg, France, and NASA's Astrophysics Data System Bibliographic Services. MS acknowledges the Postdoc@MUNI project CZ.02.2.69/0.0/0.0/16-027/0008360. PK would like to acknowledge the support from GACR international grant 17-01752J. JK and ZM were supported by grant GA ČR 18-05665S. JB and TP acknowledge VEGA 2/0031/18 and APVV 15-0458 grants. This work was supported by the Slovak Research and Development Agency under the contract No. APVV-15-0458. The research of MF was supported by the internal grant No. VVGS-PF-2018-758 of the Faculty of Science, P. J. Šafárik University in Košice. The data collection was partly funded by SAV-18-02 project.

REFERENCES

Abt H. A., Snowden M. S., 1973, *ApJS*, **25**, 137
 Bailey J. D., Landstreet J. D., Bagnulo S., 2014, *A&A*, **561**, A147
 Barros S. C. C., Demangeon O., Deleuil M., 2016, *A&A*, **594**, A100
 Bowman D. M., Buysschaert B., Neiner C., Pápics P. I., Oksala M. E., Aerts C., 2018, *A&A*, **616**, A77
 Breger M., 2000, in Breger M., Montgomery M., eds, *Astronomical Society of the Pacific Conference Series Vol. 210, Delta Scuti and Related Stars*. p. 3
 Bressan A., Marigo P., Girardi L., Salasnich B., Dal Cero C., Rubele S., Nanni A., 2012, *MNRAS*, **427**, 127
 Budaj J., 1999, *MNRAS*, **310**, 419
 Budaj J., Richards M. T., 2004, *Contributions of the Astronomical Observatory Skalnaté Pleso*, **34**, 167
 Carquillat J.-M., Priour J.-L., 2007, *MNRAS*, **380**, 1064
 Carrier F., North P., Udry S., Babel J., 2002, *A&A*, **394**, 151
 Claret A., 1999, in Gimenez A., Guinan E. F., Montesinos B., eds, *Astronomical Society of the Pacific Conference Series Vol. 173, Stellar Structure: Theory and Test of Connective Energy Transport*. p. 277

Cranmer S. R., Bastien F. A., Stassun K. G., Saar S. H., 2014, *ApJ*, **781**, 124
 Ferrario L., Pringle J. E., Tout C. A., Wickramasinghe D. T., 2009, *MNRAS*, **400**, L71
 Flower P. J., 1996, *ApJ*, **469**, 355
 Gaia Collaboration et al., 2018, *A&A*, **616**, A1
 Gandet T. L., 2008, *Information Bulletin on Variable Stars*, **5848**
 Gray R. O., Corbally C. J., 1994, *AJ*, **107**, 742
 Green G. M., et al., 2018, *MNRAS*, **478**, 651
 Heiter U., et al., 2002, *A&A*, **392**, 619
 Howell S. B., et al., 2014, *PASP*, **126**, 398
 Huber D., et al., 2016, *ApJS*, **224**, 2
 Kharchenko N. V., 2001, *Kinematika i Fizika Nebesnykh Tel*, **17**, 409
 Kochukhov O., Johnston C., Alecian E., Wade G. A., 2018, *MNRAS*, **478**, 1749
 Koubský P., Mayer P., Čáp J., Ždárský F., Zeman J., Pína L., Melich Z., 2004, *Publications of the Astronomical Institute of the Czechoslovak Academy of Sciences*, **92**, 37
 Kurtz D. W., Martinez P., 2000, *Baltic Astronomy*, **9**, 253
 Landstreet J. D., Kochukhov O., Alecian E., Bailey J. D., Mathys S., Neiner C., Wade G. A., BINAMICs Collaboration 2017, *A&A*, **601**, A129
 Lenz P., Breger M., 2005, *Communications in Asteroseismology*, **146**, 53
 Lindgren L., et al., 2018, *A&A*, **616**, A2
 Mathys G., 2017, *A&A*, **601**, A14
 Michaud G., Charland Y., Vauclair S., Vauclair G., 1976, *ApJ*, **210**, 447
 Niemczura E., Smalley B., Pych W., 2014, *Determination of Atmospheric Parameters of B-, A-, F- and G-Type Stars*, doi:10.1007/978-3-319-06956-2.
 Paunzen E., Maitzen H. M., 1998, *A&AS*, **133**, 1
 Paunzen E., et al., 2018, *A&A*, **615**, A36
 Pecaút M. J., Mamajek E. E., 2013, *ApJS*, **208**, 9
 Plavec M., Kratochvíl P., 1964, *Bulletin of the Astronomical Institutes of Czechoslovakia*, **15**, 165
 Preston G. W., 1974, *ARA&A*, **12**, 257
 Pribulla T., et al., 2015, *Astronomische Nachrichten*, **336**, 682
 Prsa A., Matijević G., Latković O., Vilardell F., Wils P., 2011, *PHOEBE: PHysics Of Eclipsing BinariEs*, *Astrophysics Source Code Library* (ascl:1106.002)
 Prvák M., Liška J., Krčička J., Mikulášek Z., Lüftinger T., 2015, *A&A*, **584**, A17
 Romanyuk I. I., 2007, *Astrophysical Bulletin*, **62**, 62
 Saar S. H., Donahue R. A., 1997, *ApJ*, **485**, 319
 Samadi R., Belkacem K., Ludwig H.-G., 2013a, *A&A*, **559**, A39
 Samadi R., et al., 2013b, *A&A*, **559**, A40
 Schöller M., Correia S., Hubrig S., Ageorges N., 2010, *A&A*, **522**, A85
 Skrutskie M. F., et al., 2006, *AJ*, **131**, 1163
 Smalley B., et al., 2015, *MNRAS*, **452**, 3334
 Tody D., 1993, in Hanisch R. J., Brissenden R. J. V., Barnes J., eds, *Astronomical Society of the Pacific Conference Series Vol. 52, Astronomical Data Analysis Software and Systems II*. p. 173
 Tutukov A. V., Fedorova A. V., 2010, *Astronomy Reports*, **54**, 156
 Zacharias N., Finch C. T., Girard T. M., Henden A., Bartlett J. L., Monet D. G., Zacharias M. I., 2013, *AJ*, **145**, 44
 van Hamme W., 1993, *AJ*, **106**, 2096

APPENDIX A: TABLES

This paper has been typeset from a $\text{\TeX}/\text{\LaTeX}$ file prepared by the author.

Table A1. Physical parameters of HD 99458 from literature and this study. The values refer to the primary component. The corresponding errors in the last digits are in parentheses. The references are: 1 – [Huber et al. \(2016\)](#), 2 – [Barros et al. \(2016\)](#), 3 – [Gaia Collaboration et al. \(2018\)](#).

T_{eff} (K)	$\log g$ (dex)	[Fe/H]	M (M_{\odot})	R (R_{\odot})	d (pc)	V_{eq} (km s^{-1})	i (deg)	$\log t$ (year)	Ref.
6623	4.05	0.001	1.487	1.843	137				1
6815									2
8199					264.7				3
7600(100)	3.70(5)	0.0+	2.15(5)	3.467(3)		64(1)	73.2(6)	8.90(5)	this study

Table A2. Relative radial velocities. In the columns Instr, OES means Ondřejov Echelle Spectrograph, while SLS means Stará Lesná Spectrograph.

HJD	V (km s^{-1})	σ (km s^{-1})	Instr	HJD	V (km s^{-1})	σ (km s^{-1})	Instr
2457828.4466	-8.5	0.8	OES	2457853.4894	26.5	3.2	OES
2457828.4679	-5.8	1.8	OES	2457853.5107	28.8	1.4	OES
2457828.4937	-4.9	0.8	OES	2457854.3795	-4.8	1.7	SLS
2457829.4223	26.9	0.8	OES	2457874.3556	-29.6	1.5	OES
2457829.4436	28.1	1.1	OES	2457874.3770	-30.0	3.4	OES
2457839.4446	-1.0	1.3	SLS	2457884.3490	-4.8	1.3	OES
2457840.4426	21.2	0.8	SLS	2457884.3599	-5.9	1.2	OES
2457841.4441	-34.5	1.4	SLS	2457884.3708	-5.4	0.8	OES
2457843.4364	1.3	1.3	SLS	2457884.3817	-5.5	1.4	OES
2457844.4162	-31.6	0.8	OES	2457891.3605	17.0	0.5	OES
2457844.4376	-30.8	2.3	OES	2457891.3819	18.1	0.9	OES
2457844.4589	-28.4	1.1	OES	2457901.3389	-40.4	1.2	SLS
2457844.4802	-27.6	1.5	OES	2457902.3264	17.9	3.1	SLS
2457844.5408	-25.7	2.1	OES	2458203.3067	-34.2	1.2	OES
2457844.5622	-22.9	4.0	OES	2458203.3280	-35.0	1.0	OES
2457844.5835	-21.8	1.8	OES	2458203.3493	-38.1	1.8	OES
2457844.6048	-21.5	0.8	OES	2458203.3905	-40.2	1.0	OES
2457845.3869	30.1	1.0	SLS	2458203.4118	-39.7	1.5	OES
2457845.4646	33.1	0.8	OES	2458226.3160	24.6	1.7	OES
2457845.4859	34.1	0.6	OES	2458226.3373	24.7	1.4	OES
2457845.5072	33.7	1.5	OES	2458227.3385	-6.9	2.0	OES
2457845.5286	33.6	1.7	OES	2458229.3268	32.7	0.2	OES
2457845.5499	33.4	1.5	OES	2458229.3481	32.7	0.4	OES
2457845.5712	32.4	1.2	OES	2458230.3165	-23.2	0.9	OES
2457846.3440	-14.4	1.0	SLS	2458230.3379	-24.6	1.9	OES
2457853.4041	25.1	0.8	OES	2458231.3301	-4.4	1.8	OES
2457853.4254	26.1	1.8	OES	2458231.3514	-4.7	1.5	OES
2457853.4467	25.9	0.5	OES	2458253.3544	12.2	1.2	OES
2457853.4681	27.8	1.4	OES	2458253.3758	14.3	1.7	OES